Observation of Microscopic CO Dynamics on Cu(001) Using ^{3}He Spin-Echo Spectroscopy

G. Alexandrowicz,* A. P. Jardine, P. Fouquet,† S. Dworski, W. Allison, and J. Ellis

Cavendish Laboratory, University of Cambridge, Madingley Road, Cambridge, CB3 0HE, United Kingdom

(Received 28 April 2004; published 7 October 2004)

We present momentum resolved measurements of quasielastic helium atom scattering made using a new ^{3}He spin-echo spectrometer. Our data for the dynamics of CO on Cu(001) indicates an activated jump mechanism which we analyze in detail using molecular dynamics simulations. A nearly isotropic potential energy surface is found with an average barrier height of ~125 meV, yielding comparable hopping rates along both the ⟨110⟩ and ⟨100⟩ directions. The measurements provide the first rigorous experimental test of state-of-the-art first-principles calculations previously made on this system.

DOI: 10.1103/PhysRevLett.93.156103 PACS numbers: 68.43.Jk, 05.10.Gg, 68.35.Ja, 68.49.Bc

Measuring adsorbate dynamics requires a technique that is sensitive to motion over the entire unit cell. Few techniques are capable of providing information about the detailed mechanism of surface diffusion, particularly the shape of the lateral adsorbate-substrate potential [1]. Since adsorbate motion involves vibration, occasionally excited to jumping between unit cells, it is preferable to use a technique that can measure the length and time scales over which an atom crosses a unit cell. Quasielastic helium atom scattering (QHAS) fulfills these criteria [1,2]. QHAS measurements, taken as a function of both momentum transfer and temperature, provide a detailed description of the system [3,4]. Due to the available experimental resolution, previous QHAS measurements were restricted to a handful of systems in which exceptionally fast diffusion occurs [3]. Recent work has also shown [5] that, without adequate energy resolution, experiments cannot distinguish between true intercell and intracell diffusion.

In this Letter, we present the first measurements showing molecular diffusion over an extended range of momentum transfer and made using an atomic beam spin-echo approach [6,7]. Spin echo extends available resolution by approximately 3 orders of magnitude, making it possible to study a much wider range of systems. The measurements presented here, on the controversial CO/Cu(001) system [8–10], were only possible through the development of the new scattering apparatus, yielding a nominal resolution for inelastic spectrum reconstruction of 2 μeV but capable of distinguishing quasielastic broadenings as small as 20 neV. The new apparatus is the first to combine the high resolution available through helium spin echo with sufficient momentum transfer and energy to map out surface processes fully [11]. Existing time of flight (TOF) measurements on CO/Cu(001) were limited to a single, high momentum transfer value [8] interpreted [5] as an activation energy for diffusion of 31 ± 10 meV, a smaller value than given by first-principles calculation [10,12]. The momentum transfer resolved data and molecular dynamics (MD) simulations presented in this Letter, combined with recent activation measurements [7], reveal a nearly isotropic potential energy surface (PES) in which surface diffusion is orders of magnitude slower than previously expected.

In the apparatus, the polarized ^{3}He beam is passed through two magnetic spin-precession fields, before and after scattering from the sample. Within the fields, the ^{3}He spins precess around the beam direction according to their velocities and the field strength. When tuned to create equal and opposite field integrals, the total accumulated phase is zero for elastic scattering and the final spin phase shift is a linear function of the energy transfer, independent, to first order, of the energy spread of the initial beam [13]. The scattered beam is eventually passed through a spin analyzer stage, which transmits the cosine spin component of the beam [14] for detection. Subtracting the constant contributions, our measured final polarization $S(\Delta\mathbf{K}, t)$ can be written

$$S(\Delta\mathbf{K}, t) \propto \int S(\Delta\mathbf{K}, \omega)\cos(t\omega)d\omega, \qquad (1)$$

where $\hbar\omega$ and $\Delta\mathbf{K}$ are the energy and momentum transferred on scattering. $S(\Delta\mathbf{K}, \omega)$, also known as the dynamic structure factor (DSF), is the probability of such an event. The spin-echo time [13], t, depends linearly on the current driving the precession coils, and the cosine transform relation in Eq. (1) allows us to scan t and reconstruct the DSF. In comparison, a TOF experiment gives a convolution of the DSF with the much wider energy distribution of the beam, masking small diffusion induced broadenings. The temporal Fourier transform of the DSF, which we measure, is also known as the intermediate scattering function (ISF), $S(\Delta\mathbf{K}, t)$. In the low coverage approximation, the ISF is the spatial Fourier transform of $G_s(R, t)$, the self pair correlation function [15], which fully describes the dynamics of the particle on the surface.

The present measurements use a single crystal Cu(100) sample cut to within 0.1 degrees of the (100) face and mechanically polished to better than 0.03 μm, followed by cleaning in ultrahigh vacuum by repeated cycling of Ar^+ sputtering (900 V, 2 μA, 15 min at 300 K) and annealing (5 min, ~850 K). The surface quality was monitored using the ^{3}He beam, ensuring a sharp specular

peak whose width corresponds to the angular resolution of the instrument ($\sim 0.1\,^\circ$), and by maintaining a high reflectivity throughout the measurements. 99.97% purity CO gas was leaked into the UHV chamber to achieve the required coverage and the sample temperature was monitored using a K-type thermocouple. The incident ^{3}He beam energy was 9.5 meV. Polarization measurements were carried out using spin-precession coil currents in the range of 0 to 7 A, giving field integrals and spin-echo times of up to 0.05 Tm and 450 ps, respectively. The measurements were fitted by assuming the usual Lorentzian quasielastic broadening [3] which leads to an exponential decay in polarization from which the width of the broadening was extracted [16]. Measurements were performed along the $\langle 100\rangle$ and $\langle 110\rangle$ crystal azimuths at a sample temperature of 190 K, using a CO overpressure of 2×10^{-6} mbar in order to stabilize a coverage of 0.1 ML. The pressure/coverage relationship was determined from a measurement of the specular reflectivity decay and $c(2 \times 2)$ diffraction peak intensity during CO dosing at 135 K. Previous adsorption studies have shown that at low temperatures, the CO coverage shows a linear dependence on the exposure, before saturating at 0.5 ML in the $c(2 \times 2)$ structure [17]. Figure 1 shows the width of the quasielastic peak in $S(\Delta\mathbf{K}, \omega)$ as a function of momentum transfer, along with an MD fit to the data described in detail below. Figure 2 shows the temperature dependence of the quasielastic broadenings. We see exceptionally small quasielastic broadenings, typically around 1 μeV, several orders of magnitude smaller than previously observable using TOF techniques. The oscillatory dependence seen in Fig. 1 immediately suggests jump diffusion [18]. We also note that the maximum broadening is the same, $\pm 10\%$, in both directions.

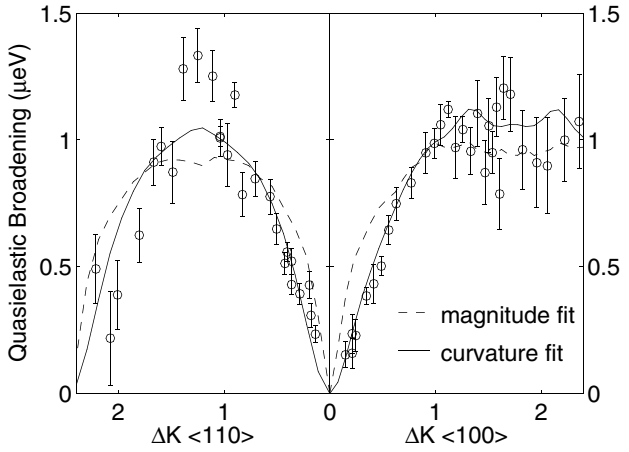

FIG. 1. Measured quasielastic peak width (FWHM) as a function of parallel momentum transfer on scattering, obtained by fitting an exponential decay to the measured polarization [16]. The sample temperature was 190 K, with a CO coverage of 0.1 ML. The $\langle 110\rangle$ and $\langle 100\rangle$ directions are shown on the left and the right of the plot, respectively. The lines show molecular dynamics fits to the data, described in the text.

For an ideal jump mechanism, the broadening induced by hopping can be related to the momentum transfer by [18]

$$\Gamma_D(\Delta\mathbf{K}) = 4\hbar\nu \sum P_j \sin^2\left(\frac{\Delta\mathbf{K}\cdot\mathbf{r}_j}{2}\right), \qquad (2)$$

where the sum is over the different possible jump sites, r is the jump distance to site j, ν is the basic attempt frequency, and P_j is the probability of a successful jump to the corresponding site. In order to gain a basic understanding of the measurements, we modeled the data using Eq. (2). Restricting CO molecules to the known adsorption sites (above the Cu atoms), we allowed single jumps over the bridge and hollow sites. The contribution to the quasielastic broadening from jumps in both crystallographic directions was accounted for by considering the projection of the jump distance along the specific axis. An exponential model was used to predict the jump probability, P_j, according to $P_j = n_j \times e^{-E_j/kT}$, where E_j is equal to E_B, the bridge site energy barrier, or E_H, the barrier at the fourfold hollow and n_j is the number of similar jumps giving equivalent projections. The resulting momentum transfer dependence for several values of the E_H/E_B ratio is shown in Fig. 3, where the relative maxima in the broadening curves is seen to provide a sensitive measure of the energy barrier ratio. Essentially, the ratio of the quasielastic broadenings reflects the ratio of potential barriers. The relative heights and oscillatory behavior in the experimental data shown in Fig. 1 can be reproduced using $E_H/E_B \sim 1$. In contrast, the activation energies and preexponents obtained from an Arrhenius plot of the temperature dependence of the quasielastic broadening are relatively insensitive to the E_H/E_B ratio and are almost identical for the $\langle 110\rangle$ and $\langle 100\rangle$ directions. On a cubic (100) surface each jump contributes a projected translation along the other crystallographic

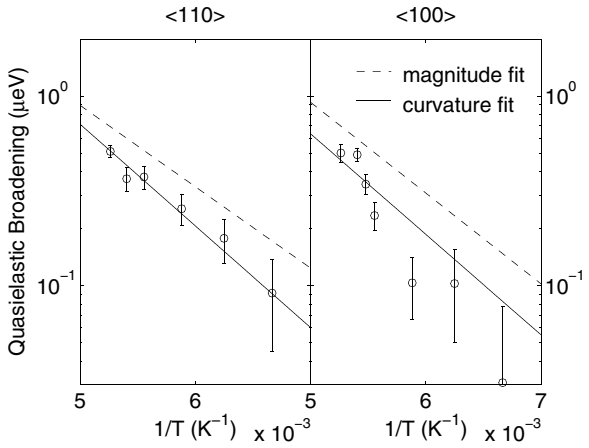

FIG. 2. Temperature dependence of the quasielastic peak width, at a momentum transfer of 0.4 Å^{-1} and a CO coverage of 0.1 ML. The $\langle 110\rangle$ [7] and $\langle 100\rangle$ measurements are shown on the left and the right sides of the graph, respectively, and the lines show molecular dynamics fits to the data.

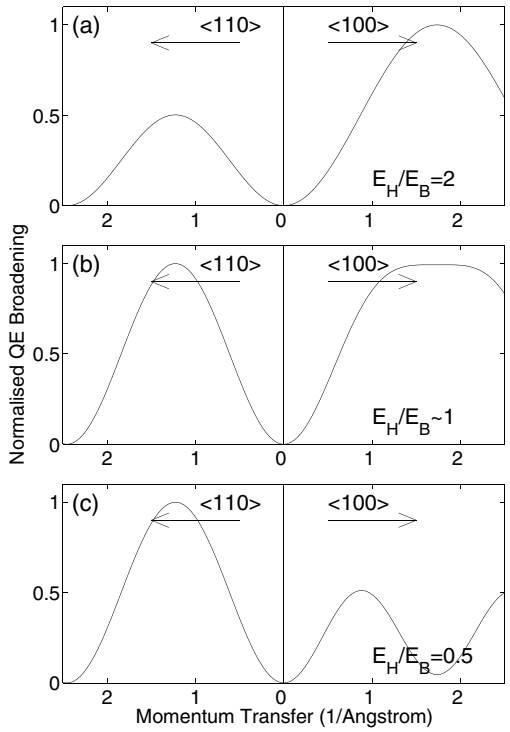

FIG. 3. Normalized calculated quasielastic peak width as a function of momentum transfer for E_H/E_B ratios of (a) 2, (b) ~1, and (c) 0.5. The ⟨110⟩ and ⟨100⟩ directions are shown on the left and the right sides of the graph, respectively. The shape and ratio of the measurements along the two directions are a sensitive measure of the relative barrier heights in the diffusion potential.

azimuth. When we increase one barrier significantly, the overall motion projected along either azimuth is mostly due to jumping over the lower barrier. Thus measuring activation energies using the conventional Arrhenius analysis reveals mainly the lower barrier value without indication of its origin.

Simple analytical models provide useful insights but are of limited use in extracting quantitative results as they neglect many important processes (intracell diffusion contributions and finite jump time, etc.). In particular, it is well established that jump activation energies extracted from an Arrhenius plot of the quasielastic broadening underestimate the adiabatic potential energy barrier, and that MD simulations are required to perform a rigorous analysis [4,5]. MD simulations also provide additional information about the energy transfer processes within the system. A complete description requires a six-dimensional quantum-dynamical calculation, including the translational, vibrational, and rotational modes [19]. In practice, QHAS data has been successfully modeled by classical motion in a two-dimensional translational potential [3,4,20,21]. We use this method to extract the important physical properties from our data. The simulations have been described in detail [20,22] and involve solving the Langevin equations of motion over a 2D trial potential, while performing a kinematic scattering calculation at each step. Frictional coupling between the adsorbate and the substrate is introduced through an Einstein model, which uses scaled random impulses from a Gaussian distribution, applied at each integration step [22]. A parameter, τ, represents the time over which the energy of the adsorbate remains correlated. The simulations are carried out in the low coverage limit and are typically run for 336 ns in 0.01 ps steps. To account for the reduction in jump possibilities due to site blocking at finite coverages, the simulated broadenings are reduced by a factor of 1.5, estimated using a geometrical, site-blocking simulation at the coverage used [23]. We chose the simplest sinusoidal potential, V_s, which allows the barriers E_B and E_H to be varied independently,

$$V_s(x, y) = \frac{1}{4}E_H\left(1 - \cos\frac{2\pi x}{a}\right)\left(1 - \cos\frac{2\pi y}{a}\right) + \frac{1}{2}E_B\left(1 - \cos\frac{2\pi x}{a}\cos\frac{2\pi y}{a}\right). \quad (3)$$

Since this potential overestimates the frustrated translation (T-mode) frequency (and the jump attempt rate), we combine it with V_a, proposed by Graham *et al.* to reproduce the T-mode data [24],

$$V_a(x, y) = \frac{1}{2}k(x^2 + y^2)[1 + u(x^2 + y^2)], \quad (4)$$

using $V(x, y) = \gamma V_a + (1 - \gamma)V_s$. To provide a smooth, circularly symmetric step transition between the two, we chose $\gamma = \exp[-\alpha((x/a)]^2 + (y/a)^2)^{\beta}$. V_a dominates the thermally explored center of the unit cell, while V_s dominates the barriers around the unit cell boundary, hence determining the diffusion. The potential is defined for $-\frac{a}{2} < x < \frac{a}{2}$ and $-\frac{a}{2} < y < \frac{a}{2}$, a is the surface lattice constant, and k and u are fixed by the T mode (95 meV/Å^2 and 0.45 Å^{-2}) [24]. The parameters $\alpha = 1000$ and $\beta = 4$ are chosen to give a smooth transition between the functions, and the precise values have a negligible effect on the simulated broadenings. The remaining parameters, E_H, E_B, and η were adjusted to reproduce the QHAS data.

The relative shapes and ratios of the momentum resolved broadenings were best reproduced with a nearly isotropic PES, giving comparable jumping over the hollow and bridge sites and supporting the discussion above. Fitting the temperature dependence of the quasielastic broadening gives potential barriers of 135 ± 20 meV over the bridge direction and 115 ± 20 meV over the hollow site [25]. The slightly lower energy barrier along the diagonal E_H compensates for the effect of a longer path, which is neglected in the analytical model.

The remaining free parameter is the frictional coupling to the surface, η. We find that, in order to reproduce the correct magnitude of broadening ("magnitude fit" in Figs. 1 and 2), we require $\eta = 1/\tau = 1/13$ ps^{-1}, suggesting that the diffusion averaged friction is ~60% weaker

than the T-mode estimate ($\eta = 1/8$ ps^{-1} [24]). These parameters achieve good agreement with the data in all respects, except for the initial curvature in Fig. 1. The discrepancy indicates that too many long jumps occur in the simulation, corresponding to higher order terms in Eq. (2). Several possibilities may account for this. Firstly, site blocking or CO-CO interactions [21] may inhibit long jumps. We rule out these effects as additional measurements at a lower coverage show the same curvature [23]. The shape of our 2D potential may also require further refinement. However, the combination of the T-mode and QHAS measurements provide quite strong constraints, making it very difficult to impose any significant changes without compromising other aspects of the overall fit. Next, we turn to the friction. An excellent fit to the curvature of the data is given by increasing the friction to $\eta = 1/2$ ps (normalized "curvature fit" in Figs. 1 and 2), but also leads to a simulated broadening which is ~ 5 times too large. Increasing the friction reduces the proportion of long jumps, but also increases the overall jump rate by increasing the rate of adsorbate/surface energy transfer. It therefore seems that position-dependent friction may resolve the problem. If the coupling to the surface increases only when the CO molecule moves away from the adsorption site, the proportion of long jumps may be reduced without also increasing the activation rate. Indeed, such variation seems quite reasonable as the molecular orientation is likely to change with position in the unit cell. Finally, the additional dimensions in the true potential may also provide an effective steric hindering of the 2D jump activation. Such effects would reduce the magnitude of the quasielastic broadening in a nonactivated way, also allowing the friction to be adjusted further. Detailed simulations will be required to resolve the relative importances of these effects and to explain the measurements fully.

Our results illustrate the success and limitations of recent first principles calculations of lateral adsorbate-surface potentials. The energy barrier along the bridge site is consistent with the potential calculated by Fouquet *et al.* [12] and with simulated temperature dependencies [26]. However, the measured barrier at the fourfold hollow is much lower than the calculated value. In fact, we believe the measured ratio of barrier heights have yet to be correctly reproduced from first principles. The newly available data provide the necessary experimental benchmarks for further theoretical progress on this prototypical surface system.

Instrumental development was supported by a Paul Instrument Fund Grant. G. A. is grateful to the Gates Cambridge Trust, Gonville & Cauis College, and an ORS fund, A. P. J. and S. D. to the Cambridge Oppenheimer Trust, and P. F. to the E.U., Humboldt Foundation and the Isaac Newton Trust.

*Electronic address: ga232@cam.ac.uk
†Present address: Institut Laue-Langevin, B.P. 156, 38042 Grenoble Cedex 9, France.

[1] J.V. Barth, Surf. Sci. Rep. **40**, 75 (2000).
[2] J.W. M. Frenken and B. J. Hinch, in *Helium Atom Scattering from Surfaces*, edited by E. Hulpke (Springer-Verlag, Berlin, 1992), Chap. 12.
[3] A. P. Jardine, J. Ellis, and W. Allison, J. Phys. Condens. Matter **14**, 6173 (2002).
[4] A. P. Graham, Surf. Sci. Rep. **49**, 115 (2003).
[5] A. P. Jardine, J. Ellis, and W. Allison, J. Chem. Phys. **120**, 8724 (2004).
[6] M. DeKieviet, D. Dubbers, C. Schmidt, D. Scholz, and U. Spinola, Phys. Rev. Lett. **75**, 1919 (1995).
[7] A. P. Jardine, S. Dworski, P. Fouquet, G. Alexandrowicz, W. Allison, and J. Ellis, Science **304**, 1790 (2004).
[8] A. P. Graham, F. Hofmann, J. P. Toennies, G. P. Williams, C. J. Hirschmugl, and J. Ellis, J. Chem. Phys. **108**, 7825 (1998).
[9] A. P. Graham and J. P. Toennies, J. Chem. Phys. **114**, 1051 (2001).
[10] Q. Ge and D. A. King, J. Chem. Phys. **114**, 1053 (2001).
[11] A. P. Jardine, P. Fouquet, J. Ellis, and W. Allison, Rev. Sci. Instrum. **72**, 3834 (2001).
[12] P. Fouquet, R. A. Olsen, and E. J. Barends, J. Chem. Phys. **119**, 509 (2003).
[13] F. Mezei, *Lecture Notes in Physics* (Springer-Verlag, Berlin, 1980), Vol. 128.
[14] S. Dworski, G. Alexandrowicz, P. Fouquet, A. P. Jardine, W. Allison, and J. Ellis, Rev. Sci. Instrum. **75**, 1963 (2004).
[15] G. H. Vineyard, Phys. Rev. **110**, 999 (1958).
[16] Static defects on the sample contribute a constant polarization component. The slow decay of the polarization within the experimental spin-echo time can be fitted with an exponential decay, plus an additional constant term of between 0% and 50% of the total signal. The constant term affects the fitted exponential decay rate and gives rise to a constant correction factor of $1.85^{+0.2}_{-0.8}$ on the absolute quasielastic energy broadening scale.
[17] J. Dvorak and H. L. Dai, J. Chem. Phys. **112**, 923 (1999).
[18] C. T. Chudley and R. J. Elliot, Proc. Phys. Soc. London **77**, 353 (1961).
[19] A. Bahel, and Z. Bacic, J. Chem. Phys. **111**, 11164 (1999).
[20] A. P. Graham, F. Hofmann, J. P. Toennies, L. Y. Chen, and S. C. Ying, Phys. Rev. B **56**, 10567 (1997).
[21] J. Ellis, A. P. Graham, F. Hofmann, and J. P. Toennies, Phys. Rev. B **63**, 195408 (2001).
[22] J. Ellis and A. P. Graham, Surf. Sci. **377-379**, 833 (1997).
[23] G. Alexandrowicz, (to be published).
[24] A. Graham, F. Hofmann, and J. P. Toennies, J. Chem. Phys. **104**, 5311 (1996).
[25] The combined form of $V(x, y)$ gives a slight dip at the hollow site, below the diffusion limiting barrier in that direction. The best fit potential parameters are $E_B = 135 \pm 20$ meV and $E_H = 95 \pm 20$ meV.
[26] J. A. Kindt, J. C. Tully, M. Head-Gordon, and M. A. Gomez, J. Chem. Phys. **109**, 3629 (1998).